Talanta 221 (2021) 121576

Contents lists available at ScienceDirect

Talanta

journal homepage: www.elsevier.com/locate/talanta

Inter-comparison of stable iron, copper and zinc isotopic compositions in six reference materials of biological origin

Lucie Sauzéat [a,b], Marta Costas-Rodríguez [c], Emmanuelle Albalat [d], Nadine Mattielli [e], Frank Vanhaecke [c], Vincent Balter [d,*]

[a] Université Clermont Auvergne, CNRS, IRD, OPGC, Laboratoire Magmas et Volcans, F-63000, Clermont-Ferrand, France
[b] Université Clermont Auvergne, CNRS, Inserm, Génétique, Reproduction et Développement, F-63000, Clermont-Ferrand, France
[c] Atomic & Mass Spectrometry – A&MS Research Unit, Department of Chemistry, Ghent University, Campus Sterre, Krijgslaan 281 - S12, 9000, Ghent, Belgium
[d] Univ Lyon, ENSL, Univ Lyon 1, CNRS, LGL-TPE, F-69007, Lyon, France
[e] Laboratoire G-Time, DGES, Université Libre de Bruxelles (ULB), Av. Roosevelt 50, CP 160/02, 1050, Brussels, Belgium

ARTICLE INFO

Keywords:
Reference material
Stable isotope
Iron
Copper
Zinc

ABSTRACT

There is a lack of certified reference materials with an organic matrix for which metal isotope ratios have been certified. Here, we have determined the iron, copper and zinc stable isotopic compositions for six reference materials of biological origin with diverse matrices, i.e. BCR-380R (whole milk), BCR-383 (beans), ERM-CE464 (tuna fish), SRM-1577c (bovine liver), DORM-4 (fish protein) and TORT-3 (lobster hepatopancreas) in three different labs. The concentrations for six major and sixteen trace elements, spanning almost four orders of magnitude, were also measured and the results obtained show an excellent agreement with certified values, demonstrating that the dissolution step was quantitative for all the standards. By taking literature data into account, 39 possible pair-wise comparisons of mean iron, copper and zinc isotopic values (δ values) could be made. Results of Tukey multiple comparisons of means yielded 11 significantly different pairs. Most of these differences are of the same order of magnitude as the estimated mean expanded uncertainties (U, $k = 2$) (±0.10‰, ±0.05‰, and ±0.05‰ for the δ^{56}Fe, δ^{65}Cu and δ^{66}Zn values, respectively). The present inter-comparison study finally proposes nineteen new preferred values for the Cu, Zn and Fe isotopic compositions of six reference materials of biological origin.

1. Introduction

Involved in a wide range of enzymes and proteins, regulating metabolic pathways and physiological processes [e.g. 1, metals including copper (Cu), iron (Fe) and zinc (Zn), are vital to the organism and any imbalance can have adverse effects on human health [e.g 2. In recent times, in addition to the determination of concentrations, the measurement of stable isotope ratios or isotopic compositions is evolving into a new tool of choice to study the metabolism of essential mineral elements in living organisms, both of plant or and animal origin. By definition, isotope fractionation refers to changes in the relative abundance of naturally occurring stable isotopes of a particular element among coexisting reservoirs hosting this element [e.g. 3. Vibrational frequencies decrease with mass commanding heavy isotopes to be enriched in coordination with the stiffest bonds, in particular those involving the oxidized form and with ligands with the stronger electronegativity (O > N > S) [3]. So far, the transition metals, iron (Fe), copper (Cu) and zinc (Zn) have been the most studied for their isotopic composition in this context.

In plants, the Fe isotopic composition (δ^{56}Fe) varies according to the type of root uptake and shows differences among plant organs [4,5]. In animals, the Fe isotopic compositions are highly fractionated between organs [6–8] and provide information on the Fe intestinal absorption efficiency [7,9–11]. In healthy conditions, the blood Fe isotopic composition of human males is different from that of pre-menopausal females [6] due to menstrual losses [12,13] and the up-regulated Fe absorption to compensate for the losses. Varying Fe isotopic composition among blood compartments signals different redox processes in red blood cells hemoglobin and in serum transferrin [14–17]. For a still unknown reason, the body mass index seems correlated with the whole blood Fe isotopic composition [16,17]. Hepatic accumulation of Fe occurs due to hereditary hemochromatosis and is reflected in the isotopic

* Corresponding author.
E-mail address: Vincent.Balter@ens-lyon.fr (V. Balter).

https://doi.org/10.1016/j.talanta.2020.121576
Received 14 May 2020; Received in revised form 16 July 2020; Accepted 11 August 2020
Available online 8 September 2020

composition of Fe in blood [18,19], while Fe dysregulations due to various etiologies resulting in anemia [20] can be scrutinized by means of the Fe isotopic compositions in whole blood and serum.

The Cu isotopes are fractionated during Cu uptake and translocation in plants [21,22]. In healthy animals, the Cu isotopes are processed slightly differently in the gut via the involvement of the microbiota [23] and Cu isotopic compositions are highly fractionated between organs [8, 24]. Similarly to Fe, the blood Cu isotopic composition is different between human males and premenopausal females due to menstrual losses and the corresponding reaction of the body to these losses [12,13]. The blood Cu isotopic composition has been shown to become lighter during ageing in a remote human Yakut population [25], and experiments on ageing *C. elegans* have confirmed this finding [26]. Copper isotopic compositions are highly sensible to disease conditions and have been investigated as a new biomarker for Wilson disease [27,28], cancer [29, 30], liver diseases [24,31] and neurodegenerative disorders [32–35].

Zinc isotopes in plants are fractionated between the organs, including roots [22,36]. Zinc isotopes are also fractionated between the organs of animals [37,38]. In humans, the blood and urine Zn isotopic composition have been suggested to reveal dietary habits [39] and more genrally, the Zn status in human [40]. The blood Zn isotopic composition has been shown to become heavier during ageing in a remote human Yakut population [25], but experiments on a worm model [26] and on a rodent model [41] did not confirm this finding. Larner et al. [42] have found different Zn isotopic compositions between breast tumors and adjacent healthy tissues, but the lack of a difference in the whole blood/serum Zn isotopic composition between breast cancer patients and healthy individuals restrains the interest in the Zn isotopic composition as a potential biomarker of cancer. Lobo et al. [30] did not reproduce the observed differences in Zn isotopic compositions between tumor and adjacent healthy tissues in oral squamous cell carcinoma. Recently, Schilling et al. [43], measured the urine Zn isotopic composition and found lower values in pancreatic ductal adenocarcinoma patients relative to healthy controls. Mouse models of neurodegenerative diseases have a brain Zn isotopic composition that is heavier than in normal wild type mice [41,44].

Determination of stable isotopic compositions of metals and the corresponding instrumentation was originally developed for the comprehension of geological problems. For quality control of the results obtained, geological reference materials were thus provided. The overall quality of the isotope ratio results depends not only on the measurement itself, but also profoundly on the sample preparation. The preparation of the sample involves the dissolution of the sample and the isolation of the metal of interest, typically by ion-exchange chromatography. Geological materials are inorganic samples with a silicate matrix containing high levels (>1%) of metals while the organic matrix of biological materials generally contains metals at trace levels only (<0.1%). The geological and biological matrices are therefore very different, and the preparation step (dissolution and target element isolation) must be adapted accordingly. As a consequence, geological reference materials cannot be used for the quality control of the processing and analysis of biological samples. To that end, the scientific community devoted to the study of metal isotopic compositions in living systems has reported isotopic values for reference biological materials. A list of the published values is given in Table S1 for Fe, Cu and Zn isotopic compositions [39,45–63]. Several observations can be drawn from that compilation. First, the Seronorm reference materials exhibit a significant isotopic heterogeneity between various lots for Fe and Cu. Second, the serum matrix seems to be, by itself, highly heterogeneous because the serum reference material BCR-639 has Cu and Zn isotopic compositions that are substantially different from those of the Seronorm materials. This holds for muscle too, because the two bovine muscle reference materials SRM-8414 and ERM-BB184 have Zn isotopic compositions differing by ~0.8‰. Third, to the best of our knowledge, there is no value published for the Fe and Cu isotopic compositions for reference materials of plant origin.

2. Experimental

The present study is an effort to fill some of the gaps that exist in the certification of isotopic compositions of biological reference materials. Here, we have determined the Fe, Cu and Zn stable isotopic compositions for five biological reference materials with a matrix of animal origin, i.e. BCR-380R (whole milk), ERM-CE464 (tuna fish), SRM-1577c (bovine liver), NRC-DORM-4 (fish protein) and NRC-TORT-3 (lobster hepatopancreas), and one biological reference material with a matrix of plant origin, BCR-383 (beans). We also have included an in-house fetal bovine serum (FBS) as a quality control sample. These isotopic compositions have been measured in three different labs, i.e. the Laboratoire de Géologie de Lyon (hereafter denoted LGL-TPE), Ecole Normale Supérieure de Lyon, France, the Atomic and Mass Spectrometry - A&MS research unit at the department of Chemistry (hereafter denoted A&MS), Ghent University, Belgium and Laboratoire G-TIME (hereafter denoted G-TIME), Université libre de Bruxelles, Belgium.

2.1. Sample description

The samples investigated consist of six biological reference materials. BCR-380R (whole milk), BCR-383 (beans) and ERM-CE464 (tuna fish) were purchased from the European Institute for Reference Materials and Measurements (IRMM), SRM-1577c (bovine liver) was purchased from the US National Institute of Standard and Technology (NIST), and DORM-4 (fish protein) and TORT-3 (lobster hepatopancreas) from the Canadian National Research Council (NRC). For all these reference materials, the homogeneity of the initial powder is warranted down to a sample size of ~100 mg by the institute in which it was prepared. Also included as a quality control sample, is a fetal bovine serum sample (FBS) sold by Sigma–Aldrich with the lot number 014M3399. The FBS material was freeze-dried and homogenized in an agate mortar. All materials were stored at the LGL-TPE. To ensure homogeneity preservation and consistent values between the different laboratories, all the reference materials were gently shaking before aliquots of at least 1g were collected and sent to the A&MS and G-TIME labs for analysis.

2.2. Sample digestion

For all sample digestions, and to avoid high measurement uncertainties due to heterogeneity of the reference material powder, a minimum sample size of 100 mg was weighed as recommended by the three institutes for reference materials.

2.2.1. LGL-TPE

All sample preparation procedures were carried out in clean laminar flow hoods using double-distilled acids to avoid any exogenous contaminations. Samples were first weighted and then dissolved in a mixture of HNO_3 (15 M) and H_2O_2 (30%) in Savillex® beakers at 120 °C for about 72 h. Attention was paid in the first hours because the mixture could be very reactive with the subsequent formation of nitric and carbon-based fumes that need to be regularly vented to avoid any overpressure. After complete dissolution, the samples were dried down and subsequently taken up with 5 mL of HNO_3 (0.5 M) from which a small aliquot was used for the quantitative determination of major and trace element concentrations.

2.2.2. A&MS

Sample preparation was performed in a class 10 clean lab. The acids used for digestion, HNO_3 (14 M) and HCl (12 M), were purified via sub-boiling distillation. Ultrapure water with a resistivity of ≥18.2 MΩ cm was obtained from an Element Milli-Q system and used for dilutions. Sample digestion was performed using HNO_3 (14 M) and H_2O_2 (30%) in closed Teflon Savillex® beakers at 110 °C for 16 h.

2.2.3. G-TIME

Sample preparation was carried out under a class-100 laminar flow hood in a class 1000 clean room. All the reagents used were purified by sub-boiling distillation and appropriate dilutions were made with 18.2 MΩ cm grade MilliQ water. To mineralize the sample, dry ashing of the sample placed in a pre-cleaned semi-opened ceramic crucible was carried out at 600 °C in a muffle furnace for 12 h. The powdered samples were transferred into a 15 mL Teflon vial (Savillex©) with 14 M HNO_3 and *suprapur* H_2O_2 at room temperature, followed by heating on a hot plate for 12–14 h. Samples were then dried down and dissolved using a 1:1 mixture of concentrated HCl and HNO_3.

2.3. Sample preparation and instrumentation

2.3.1. LGL-TPE

Iron was isolated from the concomitant matrix by ion-exchange chromatography, using a Bio-Rad column filled with 2 mL of AG 1-X8 (100–200 mesh) anionic resin. After elimination of the sample matrix with 8 mL of HCl (6 M) with traces of H_2O_2, Fe is eluted with 10 mL of HNO_3 (0.5 M). The procedure was repeated twice to ensure maximum iron purity for optimal isotope ratio measurements, leading to a total procedure blank of about 10 ng (n = 5), which generally represents 0.2 to 0.05%, and at worst 1% in the case of BCR380, of the amount of Fe present in the sample solutions prepared for isotopic analysis. After the purification, Zn remains in the iron fraction. To evaluate the effect of Zn on the measured iron isotopic compositions of the samples, we added various amounts of an elemental solution of Zn to the IRMM-014 Fe standard solution to obtain Zn/Fe ratios from 0 to 1. No deviation of the δ^{56}Fe values was observed within the analytical error (Fig. S1). The elution protocol is given in Table 1.

Copper and Zn were isolated by ion-exchange chromatography using a quartz column filled with 1.8 mL of AG MP-1 (100–200 mesh) anionic resin (Table 1). After elimination of the sample matrix with 10 mL of HCl (7 M) + H_2O_2 (0.001%), Cu and Zn were successively eluted with 20 mL of HCl (7 M) + H_2O_2 (0.001%) and 10 mL of HNO_3 (0.5 M) respectively, following the procedure described by Maréchal et al. [64]. The procedure was repeated twice leading to total procedural blanks that were on average 1.4 ng for Cu (n = 6) and 6.7 ng for Zn (n = 6), which represents in average 0.1% and 0.4% of the Cu and Zn amount, respectively, of element present in the sample solutions prepared for isotopic analysis.

The concentrations were measured following the method described in Garçon et al. [65] by ICP-OES (Thermo Scientific, iCap 6000 Radial) for major elements (Na, P, Mg, S, K and Ca) and by ICP-MS (Thermo Scientific, iCap-Q) for trace elements (Li, V, Cr, Mn, Fe, Co, Ni, Cu, Zn, As, Se, Rb, Sr, Cd, Ba and Pb). Briefly, the concentrations were calculated using calibration curves based on multi-elemental solutions. These solutions were also used to monitor and correct for the instrumental drift over the analytical session. Matrix effects and instrumental drift were also corrected for using In and Sc as internal standards for trace and major elements, respectively.

Iron isotopic compositions were measured using a Thermo Scientific Neptune Plus MC-ICP-MS at LGL-TPE. The instrument settings are given in Table 2. On the day of the measurement session, Fe purified solutions were diluted to 1 mg/L and doped with Ni used as an internal standard to monitor and correct for instrumental mass discrimination. A 1 g/L of Ni elemental standard solution from Alfa-Aesar was diluted and added to the standard and sample solutions at a concentration matching the Fe concentration, namely 1 mg/L.

The Cu and Zn isotopic compositions were measured by Nu Plasma MC-ICP-MS (Nu Instruments, Nu Plasma LR) following the procedure described by Dinis et al. [61], which is summarized in Table 2. On the day of analysis, Cu and Zn purified solutions were diluted in a Zn-doped solution (Zn JMC 3–0749L, Johnson Matthey Royston, UK) and a Cu-doped solution (Cu SRM 976, National Institute of Standards and Technology, Gaithersburg, MD, USA), respectively, to match the concentration of the standard bracketing solution (usually 300 μg/L). Measurements were carried out in static multi-collection mode and one single measurement consisted of 1 block of 30 cycles with an integration time of 10 s.

2.3.2. A&MS

After digestion, the solution was evaporated to dryness and the residue was redissolved in a mixture of HCl (8 M) and H_2O_2 (0.001%) and allowed to stand for 1 h to make sure that all of the iron and copper were in their higher oxidation states. Copper, Fe and Zn were isolated from the sample matrix using 1 mL of AG-MP1 anion exchange resin, using a revised procedure from Ref [10,20,31] (Table 1). After the sample loading and the matrix elution using 3 mL of 8 M HCl +0.001% H_2O_2, Cu, Fe and Zn were sequentially eluted using 9 mL of 5 M HCl+0.001% H_2O_2, 7 mL of 0.6M HCl and 7 mL of 0.7M HNO_3, respectively. A second chromatographic separation was applied to the Cu fraction following the same protocol to ensure the complete removal of sodium. The final purified Cu, Fe and Zn fractions were evaporated and re-dissolved in 0.5 mL of 14M HNO_3 twice to remove residual chlorides. The final residue was re-dissolved in 0.5 mL of 0.28 M HNO_3. The overall procedure led to total procedural blanks (n = 4) of about 8 ng for Fe, 0.3 ng for Cu and 3.0 ng for Zn, which represents less than 1% of the amount of each element present in the measurement solutions.

A Thermo Scientific Neptune MC-ICP-MS instrument (Germany) was used for all isotope ratio measurements. Medium mass resolution was used for all isotope ratios to avoid spectral overlap. Measurements were performed in static collection mode, using Faraday collectors connected to 10^{11} Ω amplifiers. Instrument settings and data acquisition parameters are shown in Table 2. Fe purified solutions were diluted to 300 μg/L and doped with Ni (300 μg/L) as internal standard to monitor and correct for instrumental mass discrimination. Cu and Zn solutions were adjusted to 200 μg/L and doped with Ni and Cu (both at 200 μg/L), respectively. Baseline correction was performed for each measurement sequence. The in-house elemental standards A&MS-Cu, A&MS-Fe and A&MS-Zn, previously characterized isotopically [10,20,31], were included every 5 samples for quality assurance/quality control (QA/QC) of the isotope ratio measurements.

2.3.3. G-TIME

After complete dissolution, solutions were evaporated to dryness at 125 °C and HCl (6 M) was added to convert the metals into their chloride form prior to the chromatographic separation. Isolation of Zn was realized using a 2 mL Bio-Rad column loaded with pre-cleaned AG1-X8 100–200 mesh resin (analytical grade, chloride form) following a modified elution protocol from Maréchal et al. [64] (see details in

Table 1
Ion exchange protocols for the chromatographic separation of Cu, Fe and Zn.

Lab	LGL-TPE		A&MS	G-TIME
Element	Fe	Cu, Zn	Cu, Fe, Zn	Zn
Column	Bio Rad	Quartz	Bio Rad	Bio-Rad
Resin	2 mL AG 1-X8	1.8 mL AG MP-1	1 mL AG MP-1	2 mL AG 1-X8
Matrix	8 mL HCl (6M)	10 mL HCl (7 M) + H_2O_2 (0.001%)	3 mL HCl (8 M) + H_2O_2 (0.001%)	4 mL HCl (6M) + H_2O_2 (0.001%)
Cu elution		20 mL HCl (7 M) + H_2O_2 (0.001%)	9 mL HCl (5 M) + H_2O_2 (0.001%)	
Fe elution	10 mL HNO_3 (0.5 M)	13 mL HCl (2 M) + H_2O_2 (0.001%)	7 mL HCl (0.6 M)	
Zn elution		10 mL HNO_3 (0.5 M)	7 mL HNO_3 (0.7 M)	15 mL HNO_3 (1 M) + HBr (0.1 M)

Table 2
Instrument settings and data acquisition parameters for MC-ICP-MS analysis.

Lab	LGL-TPE		A&MS			G-TIME
Element (+ internal standard)	Fe (+Ni)	Cu (+Zn), Zn (+Cu)	Fe (+Ni)	Cu (+Ni)	Zn (+Cu)	Zn (+Cu)
MC-ICP-MS	Neptune	Nu Plasma	Neptune	Neptune	Neptune	Nu Plasma
RF power (W)	1200	1350	1200	1200	1200	1350
Plasma condition	wet, quartz cyclonic/scott double spray chamber	wet, cyclonic spray chamber	wet, cyclonic/scott double spray chamber	wet, cyclonic/scott double spray chamber	wet, cyclonic/scott double spray chamber	wet, cyclonic spray chamber
Sample uptake rate (mL min-1)	100	100	100	100	100	80–100
Coolant Ar flow (L min-1)	15	13.5	15	15	15	15
Auxiliary Ar flow (L min-1)	0.7–1.1	1.25	0.75–0.85	0.75–0.85	0.75–0.85	0.90
Nebulizer Ar flow (L min-1)	0.9–1.1	1	1.03–1.08	1.03–1.08	1.03–1.08	0.86
Mass resolution	4000 (or 10,000)	300	4000 (or 10,000)	4000	4000	300
Sampling cone	Ni Jet, ø = 1.1 mm	Ni	Ni Jet, ø = 1.1 mm	Ni Jet, ø = 1.1 mm	Ni Jet, ø = 1.1 mm	Ni
Skimmer cone	Ni H-type, ø = 0.8 mm	Ni H-type	Ni H-type, ø = 0.8 mm	Ni H-type, ø = 0.8 mm	Ni H-type, ø = 0.8 mm	Ni WA6
Cup configuration	H3: ^{62}Ni; H1: ^{60}Ni; L1: ^{57}Fe; L2: ^{56}Fe; L4: ^{54}Fe	H5: ^{69}Ga; H4: ^{68}Zn; H3: $^{67.5}$; H2: ^{67}Zn; Ax: ^{66}Zn; L1: $^{65.5}$; L2: ^{65}Cu; L3: ^{64}Zn; L4: ^{63}Cu; L5 ^{62}Ni	H3: ^{62}Ni; H1: ^{60}Ni; Ax: ^{58}(Fe + Ni); L1: ^{57}Fe; L2: ^{56}Fe; L4: ^{54}Fe	H3: ^{65}Cu; H1: ^{63}Cu; Ax: ^{62}Ni; L1: ^{61}Ni; L3: ^{60}Ni	H2: ^{68}Zn; H1: ^{67}Zn; Ax: ^{66}Zn; L1: ^{65}Cu; L2: ^{64}Zn; L3: ^{63}Cu	H6: ^{68}Zn; H4: ^{67}Zn; H2: ^{66}Zn; Ax: ^{65}Cu; L2: ^{64}Zn; L4: ^{63}Cu; L5: ^{62}Ni
Sensitivity	1 ppm ~ 12.5 V FeT	0.3 ppm ~ 7 V CuT ~ 5 V ZnT	0.3 ppm–15 V	0.2 ppm ~ 15 V	0.2 ppm–2.5 V	0.5 ppm ~ 7 V CuT
Blank signal (2% HNO_3)	^{56}Fe ~ 10 mV	^{63}Cu ~ 0.1 mV	<0.01%	<0.01%	<0.05%	^{64}Zn ~ 0.5 mV
Integration time (s)	10	10	4.194	4.194	4.194	10
Cycles	30	30	45	45	45	60

Ref. [66]). The sample is re-dissolved in 1 mL of 6 M HCl with 20 µl of 30% H_2O_2 before loading on the column. The matrix, Cu and Fe were discarded using HCl (8 M) followed by HCl (0.5 M), and Zn was eluted with 15 mL of 1 M HNO_3 + 0.1 M HBr (Table 2). Total procedural blanks (digestion and chromatography) were less than 10 ng of Zn. Dried Zn fractions were redissolved in 100 µL of concentrated HNO_3 and then diluted at 400 µg/L in 0.05M HNO_3 for isotope ratio measurements. Cu standard solution was systematically added to samples and standards as an internal standard with identical concentrations (400 µg/L). Zinc isotopes ratios were measured on a Nu Plasma II HR MC-ICP-MS (Nu Instruments) with the instrumental settings as given in Table 3. All Zn and Cu masses (^{64}Zn, ^{66}Zn, ^{67}Zn, ^{68}Zn, ^{70}Zn and ^{63}Cu, ^{65}Cu) were monitored, as well as ^{62}Ni to correct for interference between ^{64}Ni and ^{64}Zn. However, the ^{62}Ni beam intensity was systematically lower than the background signal ($\leq 1.10^{-4}$ V). The signals were measured by static multi-collection. A single measurement consisted of a measurement of 60 cycles, i.e. 3 blocks of 20 cycles (with an integration time of 10 s, each). On-peak baseline measurement with 30 s integration time was done prior to each analysis using a 0.05 M HNO_3 acid blank, and the value obtained is then subtracted on-line during the analytical sequence for all the samples/standards.

In all labs and for all isotope ratios measurements, instrumental mass discrimination and temporal drift were corrected with an exponential law using an admixed element as internal standard, combined with sample-standard bracketing, as recommended by Maréchal et al. [64]. The doping conditions are given in Table 2. All the results of isotopic ratios measurements are given in the delta annotation (expressed in ‰) and reported relative to the international isotopic standard solutions NIST IRMM-014 for Fe, SRM-976 for Cu and JMC 3–0749L for Zn using the following equations:

$$\delta^{56}Fe = \left[\frac{\left(^{56}Fe/^{54}Fe\right)_{sample}}{\left(^{56}Fe/^{54}Fe\right)_{standard}} - 1\right] \times 1000 \quad (1)$$

$$\delta^{65}Cu = \left[\frac{\left(^{65}Cu/^{63}Cu\right)_{sample}}{\left(^{65}Cu/^{63}Cu\right)_{standard}} - 1\right] \times 1000 \quad (2)$$

Table 3
Linear regression parameters for the observed mass fractionations. The theoretical slope (β) values are given for kinetically and thermodynamically controlled mass fractionations for comparison.

Lab				LGL-TPE	A&MS	G-TIME
$d^{57}Fe$ vs $d^{56}Fe$	Measured	Intercept		0.027 (±0.019)	−0.003 (±0.021)	
		Slope (b)		1.486 (±0.015)	1.422 (±0.018)	
	Theoretical b	Equilibrium	1.475			
		Kinetic	1.488			
$d^{67}Zn$ vs $d^{66}Zn$	Measured	Intercept		0.010 (±0.011)	0.013 (±0.008)	0.067 (±0.014)
		Slope (b)		1.515 (±0.023)	1.484 (±0.019)	1.427 (±0.031)
	Theoretical b	Equilibrium	1.479			
		Kinetic	1.490			
$d^{68}Zn$ vs $d^{66}Zn$	Measured	Intercept		0.018 (±0.006)	0.002 (±0.007)	−0.033 (±0.016)
		Slope (b)		1.967 (±0.012)	1.948 (±0.016)	1.985 (±0.034)
	Theoretical b	Equilibrium	1.942			
		Kinetic	1.971			

$$\delta^{66}Zn = \left[\frac{\left(^{66}Zn/^{64}Zn\right)_{sample}}{\left(^{66}Zn/^{64}Zn\right)_{standard}} - 1 \right] \times 1000 \quad (3)$$

All statistical analyses was performed using the R software [67].

3. Results

3.1. Uncertainty estimation for mass fractions

The uncertainties given in the present work are expanded uncertainties (denoted U), obtained by multiplying the combined standard uncertainty $u_c(y)$ of the estimate y by a coverage factor k such that $U = ku_c(y)$ with $k = 2$ corresponding to a level of confidence of about 95%. Following the recommendations of the Guide to the expression of uncertainty in measurement [68], identified sources of uncertainty (x) for the measurement of mass fractions (y) relate to instrumental (variable background stability and counting efficiency) and analytical (error in mass and volume measurements, contamination). The determination of the combined standard uncertainty can be thus considered as a linear combination of terms representing the variation of the output estimate y generated by the uncertainty of each input estimate x such that:

$$u_c^2(y) = \left[\sum_{i=1}^{N} c_i u(x_i) \right]^2 \quad (4)$$

where $u_c(y)$ is the combined uncertainty; c_i the sensitivity coefficient and $u(x_i)$ the standard uncertainty which can be estimated by using the standard deviation calculated form replicate measurements. Here, the sensitivity coefficients were the same for all the measurements and were not further considered.

Excluding contamination as a significant source of uncertainty because the contribution of the procedural blanks was negligible and all samples were processed in a clean room, other analytical uncertainties can be considered insignificant compared to instrumental uncertainties associated with the ICP-MS or ICP-OES techniques, which are at best <5% (RSD). Comparison of expanded uncertainties for the determination of major elements (n = 18) and trace elements (n = 36) are of the same order of magnitude as those determined by NIST, IRMM and NRC (Fig. S2).

3.2. Determination of mass fractions

The results of the determination of mass fractions are given in Table S2. The number of measurements (n) correspond to the number of aliquots of digested reference materials measured one time. The table also includes the certified values (C_v) when available, allowing to calculate an accuracy (%) of the measurements (M_v) given the relationship:

$$\text{accuracy } \% = 100 - [100.(C_v \ M_v) / C_v] \quad (5)$$

For all the reference materials and all the elements, the calculation of the accuracy (n = 54) showed that the majority of the results have an accuracy > 90% (median = 93.0%), with two outliers, K in DORM-4 (69.5%) and Ni in SRM-1577c (47.8%), resulting in a mean accuracy value of 91.5% (Fig. 1). The overall comparison of the measured values and the certified values showed a very significant correlation ($p < 2e^{-16}$ ***, n = 54), spanning more than four orders of magnitude of mass fraction, a slope close to unity (0.993 ± 0.006) and a small offset of 0.383 ± 0.612 at origin (Fig. 2). The close agreement between measured and certified values whether for trace or major elements, demonstrates that the digestion step was quantitative at LGL-TPE. By extension to the other uncertified mass fractions, the present study allows to propose sixty-three new mass fraction values, i.e. sixteen for BCR-380R, thirteen for BCR-383, three for DORM-4, twenty for ERM-CE464, one for SRM-1577c and ten for TORT-3 (Table S2). These proposed new values are particularly of interest for the reference materials provided by IRMM (BCR-380R, BCR-383 and ERM-CE464) which are poorly characterized in terms of elemental mass fractions.

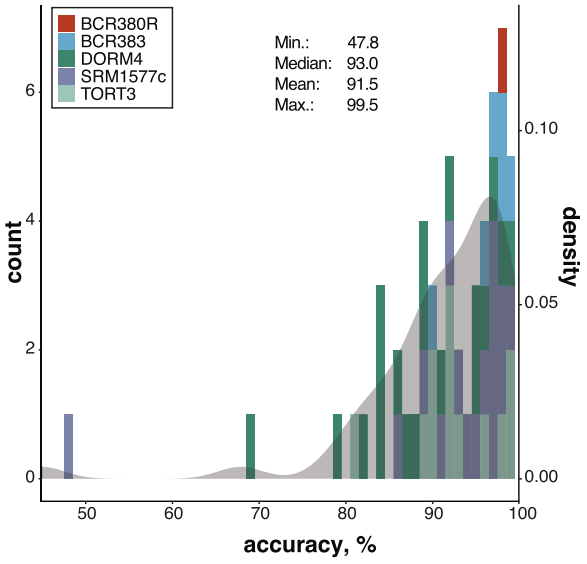

Fig. 1. Distribution of mass fraction values accuracy (%) in reference materials from this study. The summary of the distribution parameters is indicated. The grey shaded area corresponds to the density of the distribution of the accuracy of the results.

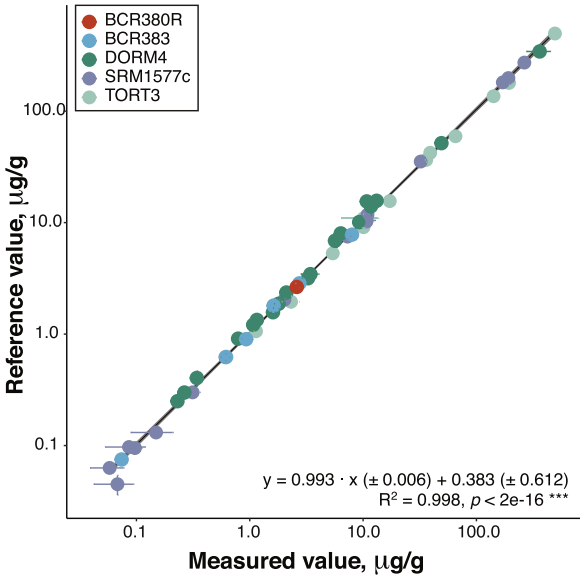

Fig. 2. Correlation between certified and measured mass fraction values (µg/g) in the reference materials analyzed in this study. The linear regression parameters are indicated along with the correlation coefficient and the associated p value. Error bars are U (k = 2).

3.3. Uncertainty estimation for isotopic compositions

The calculation of the combined standard uncertainty $u_c(y)$ for an isotope ratio can also be considered as a linear combination of terms of variations, but the calculation of the combined standard uncertainty of the delta value involves the uncertainties of the isotope ratios of the sample and those of the bracketing standard. A full demonstration of the calculation of the combined standard uncertainty of the delta value (δ) is provided by Sullivan et al. [51] and the final equation is given here for a

symbolic $r^{A/a}$ isotope ratio:

$$u^2(\delta) = \left(\frac{1}{r^{A/a}_{std}}\right)^2 \cdot u^2\left(r^{A/a}_{spl}\right) + \left(-\frac{r^{A/a}_{spl}}{r^{A/a^2}_{std}}\right)^2 \cdot u^2\left(r^{A/a}_{std}\right) \quad (6)$$

where the subscripts *std* and *spl* stand for the standard and the sample, respectively and u (r) is the standard uncertainty for the measured ratio, which can be estimated by using the standard deviation calculated from replicate measurements. We have calculated the expanded uncertainties U for the δ^{56}Fe, δ^{57}Fe, δ^{65}Cu, δ^{66}Zn, δ^{67}Zn and δ^{68}Zn values which are given in Tables S3–S9 along with the corresponding isotope ratios. The estimated mean expanded uncertainties were ±0.10‰ for the δ^{56}Fe value, and ±0.05‰ for the δ^{65}Cu and δ^{66}Zn values. The magnitude of the expanded uncertainties for the δ^{65}Cu value is close to that reported by Sullivan et al. [51], i.e. ± 0.07‰. For the Fe isotopic compositions, the higher U value is due to the fact that some reference materials (BCR-383, ERM-CE464 and one sample of FBS) at LGL-TPE exhibited enhanced instability. Reported error values in the present paper are therefore expanded uncertainty U with a coverage k factor of two, unless specified otherwise.

3.4. Determination of isotopic compositions

All results are given in table Tables S3–S9. One aspect of the quality of the isotopic results is assessed by the calculation of the exponent β relating the mass-dependent fractionation factors for two isotope ratios, which is different for kinetically and thermodynamically controlled fractionation [69]. Plots of δ^{57}Fe vs δ^{56}Fe (Fig. 3A), δ^{67}Zn vs δ^{66}Zn (Fig. 3B), and δ^{68}Zn vs δ^{66}Zn (Fig. 3C) yield the mass fractionation relationships in three-isotope spaces, allowing to calculate the β values, which correspond to the slopes of the respective best-fit linear regressions. Comparison with theoretical values (Table 3) show excellent agreement. In biological systems, mass fractionation is suspected to be under kinetic control, but the calculated β values do not show characteristics of kinetic mass fractionation (Table 3), probably because the fractionation per mass unit is too small, i.e. < 3‰ estimated by Young et al. [69] using magnesium isotope ratios.

Overall, we have considered as valid isotopic data sixty-four measurements of δ^{56}Fe values (LGL-TPE, $n = 30$, A&MS, $n = 34$), eighty-nine measurements of δ^{65}Cu values (LGL-TPE, $n = 57$, A&MS, $n = 32$) and one hundred measurements of δ^{66}Zn values (LGL-TPE, $n = 60$, A&MS, $n = 34$, G-TIME, $n = 6$).

4. Discussion

The results of Craddock and Dauphas [53] for the Fe isotopic composition of the SRM-1577c reference material ($n = 1$) and those of Sullivan et al. [51] for the Cu isotopic compositions of the DORM-4 ($n = 6$) and TORT-3 ($n = 6$) reference materials can be merged with the present results ($n = 253$). In order to determine preferred isotopic values, pair-wise comparisons of the mean isotope ratios have been performed using Tukey's HSD tests. A non-significant associated p value (>0.05) indicates that the means compared are not different, while an associated p value <0.05 indicates that the means compared are significantly different. All the results of the possible pair-wise comparisons are given in Table S10. Of thirty-nine comparisons, eleven means were significantly different, with a bias between them ranging from 0.06‰ to 0.25‰, with an average value of 0.09‰ (Table S10). However, most of the differences between the mean values are of the same order of magnitude as the calculated expanded uncertainties, i.e. ± 0.10‰, ±0.05‰, and ±0.05‰ for the δ^{56}Fe, δ^{65}Cu and δ^{66}Zn values, respectively. Taking the expanded uncertainties into account, only two differences remain significant, which are between LGL-TPE and A&MS labs for the δ^{65}Cu value of the BCR-380R reference material (0.25‰) and between LGL-TPE and G-TIME labs for the δ^{66}Zn value of the ERM-CE464 reference material (0.14‰). These discrepancies might be

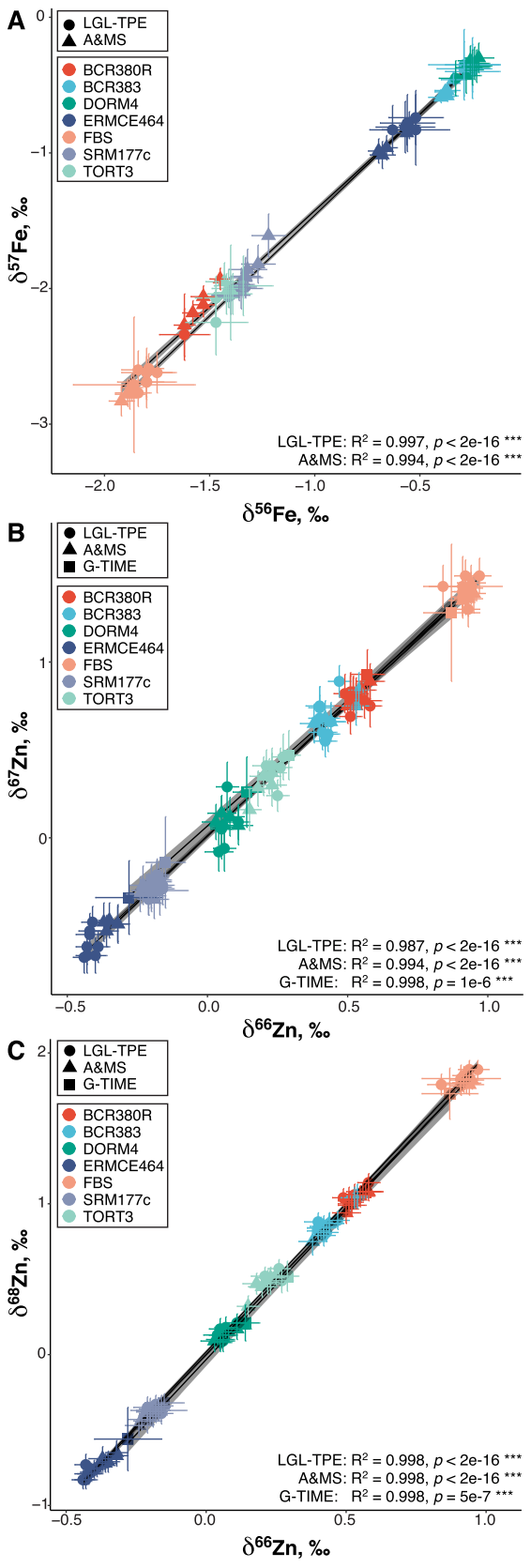

Fig. 3. Mass fractionation in three-isotope space for the reference materials analyzed in this study; A) δ^{57}Fe vs δ^{56}Fe; B) δ^{67}Zn vs δ^{66}Zn; C) δ^{68}Zn vs δ^{66}Zn. In all cases, the correlation coefficient and the associated p value are indicated. The linear regression parameters are given in Table 3. Error bars are U ($k = 2$).

explained by incomplete digestion of lipid compounds present in the samples, notably significant for the BCR-380R and ERM-CE464 reference materials which have a lipid content up to 27 wt%.

The final results are shown in Figs. 4–6 for the δ^{56}Fe, δ^{65}Cu and δ^{66}Zn values, respectively. The δ^{56}Fe values range from −1.92‰ to ~ −0.22‰, representing a span of variation of 0.85‰ per mass unit (Fig. 4). The range of variation is 0.75‰ per mass unit for the δ^{65}Cu values (min. = −0.15‰, max. = 1.32‰, Figs. 5) and 0.70‰ per mass unit for the δ^{66}Zn values (min. = −0.44‰, max. = 0.97‰, Fig. 6).

The δ^{56}Fe value for the SRM-1577c reference material reported by Craddock and Dauphas [53] is −1.34 ± 0.03‰ (±2SD), in accordance with the values determined at LGL-TPE (−1.36 ± 0.06‰) and A&MS (−1.29 ± 0.08‰) (Table S8). The present Fe isotopic composition complements well the reduced variability already measured on whole blood reference materials, which permanently exhibit very low δ^{56}Fe values < −2‰ (Table S1). The DORM-4 reference material displays the highest δ^{56}Fe value determined here (−0.26 ± 0.07‰, Fig. 4). DORM-4 is a fish protein homogenate, but it is not specified whether it was prepared from a freshwater or a seawater fish. The Fe isotopic compositions of the tuna fish muscle ERM-CE464 reference material (−0.60 ± 0.09‰, Fig. 4) and the already measured shrimp and tuna muscles [6] exhibit slightly negative values, suggesting that the DORM-4 reference material was likely prepared from seawater fish. Note that the TORT-3 reference material, which is also produced from a seawater animal (lobster), has a negative δ^{56}Fe value (−1.41 ± 0.10‰), showing that the Fe isotope fractionation between organs is probably important in the entire animal kingdom. Regarding plants, the bean BCR-383 reference material also has a slightly negative δ^{56}Fe value (−0.33 ± 0.09‰, Fig. 4), in accordance with the values found by Walczyk and von Blanckenburg [6].

The δ^{65}Cu values for the DORM-4 reference material reported by Sullivan et al. [51] is 0.52 ± 0.06‰, in accordance with the values determined at LGL-TPE (0.47 ± 0.04‰) and A&MS (0.45 ± 0.04‰)

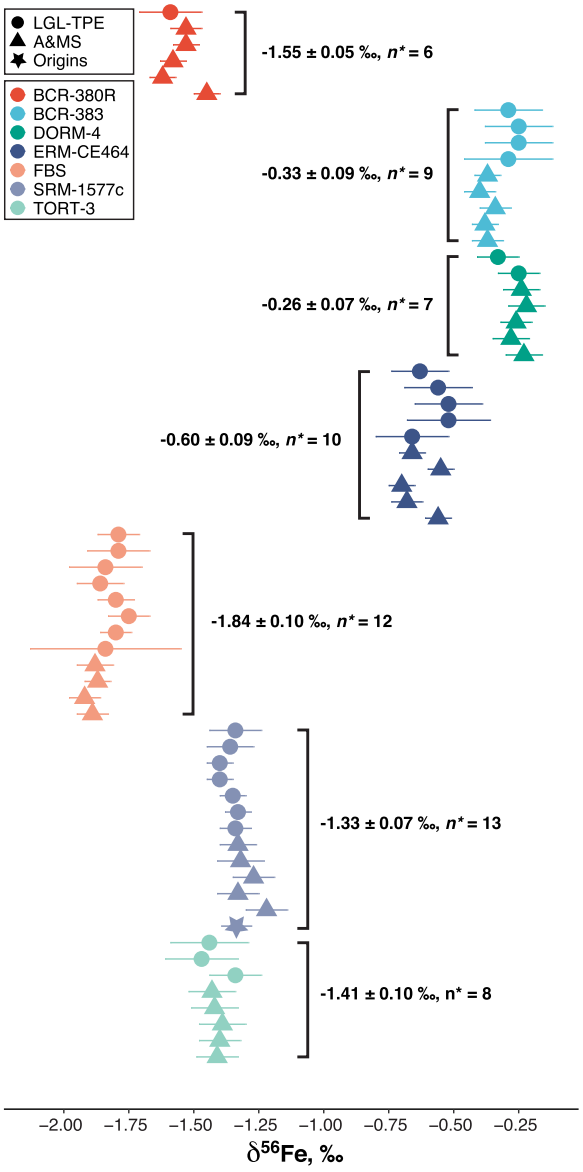

Fig. 4. Distribution of the δ^{56}Fe values in reference materials analyzed in this study. Preferred δ^{56}Fe values are indicated. Error associated to the preferred value is the mean of U (k = 2) for each aliquot digested and processed according to the chromatographic procedure. The n^* value corresponds to the number of these aliquots. Error bars are U (k = 2). Origins stands for the lab of Craddock and Dauphas [53].

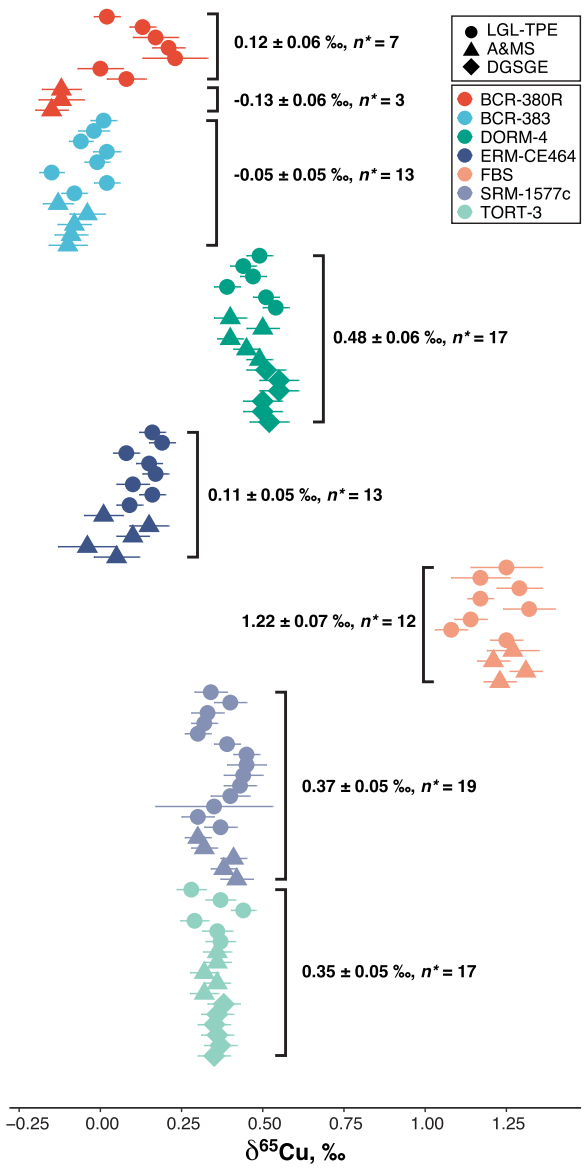

Fig. 5. Distribution of the δ^{65}Cu values in reference materials analyzed in this study. Preferred δ^{65}Cu values are indicated. Error associated to the preferred value is the mean of U (k = 2) for each aliquot digested and processed according to the chromatographic procedure. The n^* value corresponds to the number of these aliquots. Error bars are U (k = 2). DGSGE stands for the lab (Department of Geological Sciences and Geological Engineering) of Sullivan et al. [51].

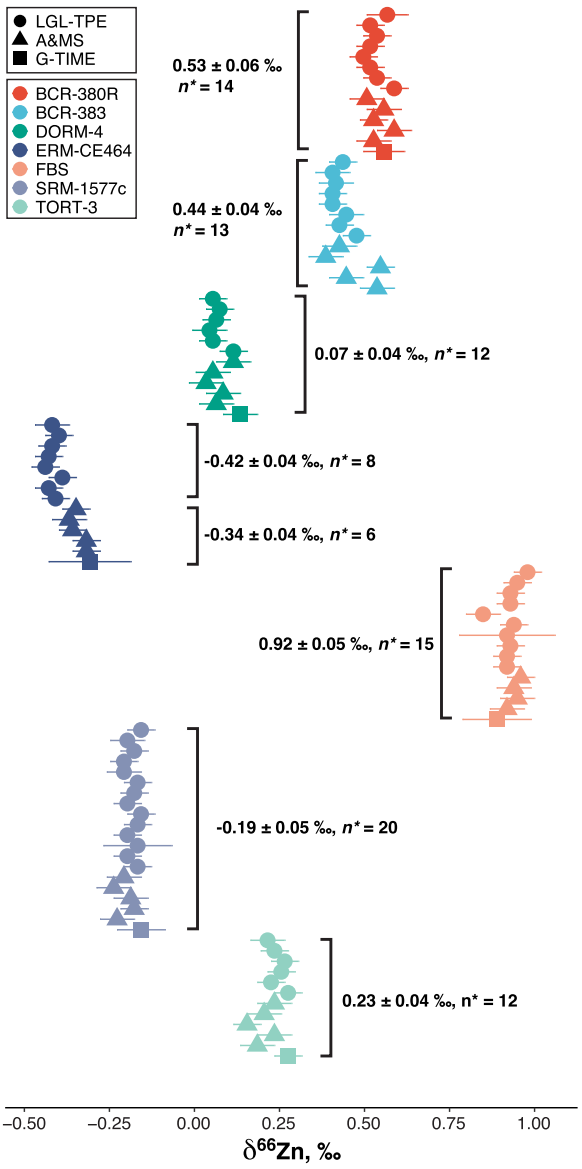

Fig. 6. Distribution of the δ^{66}Zn values in reference materials analyzed in this study. Preferred δ^{66}Zn values are indicated. Error associated to the preferred value is the mean of *U* (k = 2) for each aliquot digested and processed according to the chromatographic procedure. The *n** value corresponds to the number of these aliquots. Error bars are *U* (*k* = 2).

(Table S5). This also holds for the δ^{65}Cu value of the TORT-3 reference material which was measured at 0.35 ± 0.04‰ at LGL-TPE, 0.34 ± 0.04‰ at A&MS, and 0.36 ± 0.05‰ at DGSGE (Table S9). The δ^{65}Cu values obtained in the present study are within the range of those already reported for this reference material (Table S1). The FBS serum material, used as a quality control sample and not a reference material, shows a high δ^{65}Cu value (1.22 ± 0.07‰, Fig. 5). The fish protein DORM4 reference material has a δ^{65}Cu value of 0.48 ± 0.06‰, different from that of the dogfish liver DOLT-5 (−0.02 ± 0.08‰, ±2SD) (Table S1), which demonstrates that isotope fractionation among organs of lower vertebrates also takes place for Cu. Regarding plant, the δ^{65}Cu value of the bean BCR-383 reference material is close to 0‰ (−0.05 ± 0.05‰, Fig. 5).

The δ^{66}Zn values determined in the present study are situated within the range of the values already published for reference materials, i.e. between −0.4‰ and 1.1‰ (Table S1). BCR-639 exhibits a very negative value (~-3‰ [42,52], Table S1), which is unusual regarding the known Zn isotopic variability. The BCR-639 reference material is a "high-level" serum that has been doped with trace elements, and we think that it contains added Zn, probably highly purified Zn, with a negative δ^{66}Zn value (Rehkämper M., Pers. Comm.). As for Cu, the FBS serum material has a high δ^{66}Zn value (0.92 ± 0.05‰, Fig. 6). The other biological reference materials of animal origin show δ^{66}Zn values ranging from ~ −0.3‰ for the tuna fish muscle ERM-CE464 to ~ +0.5‰ for the whole milk BCR-380R, probably produced from cow milk (Fig. 6).

The results presented in this paper may be helpful for those researchers exploring high-precision isotopic analysis of Cu, Fe and/or Zn in biological and clinical sciences, providing them with a precious and sensitive tool for the quality control of their results.

Authors-credit

Lucie Sauzéat: investigation, resources, data curation, writing - review & editing; Marta Costas-Rodríguez: investigation, resources, data curation, writing - review & editing; Emmanuelle Albalat: investigation, resources, data curation, writing - review & editing; Nadine Mattielli: investigation, resources, data curation, writing - review & editing; Frank Vanhaecke: writing - review & editing, supervision; Vincent Balter: conceptualization, formal analysis, data curation, writing original draft, review and editing, supervision, project administration.

Declaration of competing interest

The authors declare that they have no known competing financial interests or personal relationships that could have appeared to influence the work reported in this paper.

Acknowledgements

V.B. and L.S. are grateful to Fondation Bullukian, Fondation Mérieux, the CNRS Mission pour l'Interdisciplinarité as well as the Ecole Polytechnique Fédérale of Lausanne (P. Gillet) for their financial support. Lu Yang is thanked for sharing the raw Cu isotopic data of the DORM-4 and TORT-3 reference materials. M.C.-R. acknowledges the Flemish Research Foundation (FWO) for her postdoctoral grant. F.V. acknowledges FWO for providing the funding for the acquisition of MC-ICP-MS instrumentation (ZW15-02 – G0H6216N). NM thanks Jeroen de Jong and Wendy Debouge for their assistance during the analytical work. NM acknowledges the F.R.S-FNRS for its precious financial support in the G-Time instrumental platform development.

Appendix A. Supplementary data

Supplementary data to this article can be found online at https://doi.org/10.1016/j.talanta.2020.121576.

References

[1] K.J. Waldron, N.J. Robinson, How do bacterial cells ensure that metalloproteins get the correct metal? Nat. Rev. Microbiol. 7 (2009) 25–35.
[2] K.J. Barnham, A.I. Bush, Biological metals and metal-targeting compounds in major neurodegenerative diseases, Chem. Soc. Rev. 43 (2014) 6727–6749.
[3] F. Albarède, P. Télouk, V. Balter, Medical applications of isotope metallomics. Measurements, theories and applications of non-traditional stable isotopes, Rev. Mineral. Geochem. 82 (2017) 851–885.
[4] M. Guelke, F. von Blanckenburg, Fractionation of stable iron isotopes in higher plants, Environ. Sci. Technol. 41 (2007) 1896–1901.
[5] M. Kiczka, J.G. Wiederhold, S.M. Kraemer, B. Bourdon, R. Kretzschmar, Iron isotope fractionation during Fe uptake and translocation in alpine plants, Environ. Sci. Technol. 44 (2010) 6144–6150.
[6] T. Walczyk, F. von Blanckenburg, Natural iron isotope variations in human blood, Science 295 (2002) 2065–2067.
[7] K. Hotz, H. Augsburger, T. Walczyk, Isotopic signatures of iron in body tissues as a potential biomarker for iron metabolism, J. Anal. At. Spectrom. 26 (2011) 1347–1353.
[8] V. Balter, A. Lamboux, A. Zazzo, P. Télouk, Y. Leverrier, J. Marvel, A.P. Moloney, F. J. Monahan, O. Schmidt, F. Albarède, Contrasting Fe, Cu, and Zn isotopic patterns

in organs and body fluids of mice and sheep, with emphasis on cellular fractionation, Metall 5 (2013) 1470–1482.
[9] K. Hotz, T. Walczyk, Natural iron isotopic composition of blood is an indicator of dietary iron absorption efficiency in humans, J. Biol. Inorg. Chem. 18 (2013) 1–7.
[10] L. Van Heghe, E. Engström, I. Rodushkin, C. Cloquet, F. Vanhaecke, Isotopic analysis of the metabolically relevant transition metals Cu, Fe and Zn in human blood from vegetarians and omnivores using multi-collector ICP-mass spectrometry, J. Anal. At. Spectrom. 27 (2012) 1327–1334.
[11] M.R. Flórez, Y. Anoshkina, M. Costas-Rodríguez, C. Grootaert, J. Van Camp, J. Delanghe, F. Vanhaecke, Natural Fe isotope fractionation in an intestinal Caco-2 cell line model, J. Anal. At. Spectrom. 32 (2017) 1713–1720.
[12] L. Van Heghe, O. Deltombe, J. Delanghe, H. Depypere, F. Vanhaecke, The influence of menstrual blood loss and age on the isotopic composition of Cu, Fe and Zn in human whole blood, J. Anal. At. Spectrom. 29 (2014) 478–482.
[13] K. Jaouen, V. Balter, Menopause effect on blood Fe and Cu isotope compositions, Am. J. Phys. Anthropol. 153 (2014) 280–285.
[14] F. Albarède, P. Télouk, A. Lamboux, K. Jaouen, V. Balter, Isotopic evidence of unaccounted for Fe and Cu erythropoietic pathways, Metall 3 (2011) 926–933.
[15] F. von Blanckenburg, M. Oelze, D.G. Schmid, K. van Zuilen, H.P. Gschwind, A. J. Slade, S. Stitah, D. Kaufmann, P. Swart, An iron stable isotope comparison between human erythrocytes and plasma, Metall 6 (2014) 2052–2061.
[16] Y.-H. Liang, K.-Y.A. Huang, D.-C. Lee, K.-N. Pang, S.-H. Chen, High-precision iron isotope analysis of whole blood, erythrocytes, and serum in adults, J. Trace Elem. Med. Biol. 58 (2020) 126421.
[17] J.C. Cikomola, M.R. Flórez, M. Costas-Rodríguez, Y. Anoshkina, K. Vandepoele, P. B. Katchunga, A.S. Kishabongo, M.M. Speeckaert, F. Vanhaecke, J.R. Delanghe, Whole blood Fe isotopic signature in a sub-Saharan African population, Metall 9 (2017) 1142–1149.
[18] P.-A. Krayenbuehl, T. Walczyk, R. Schoenberg, F. von Blanckenburg, G. Schulthess, Hereditary hemochromatosis is reflected in the iron isotope composition of blood, Blood 105 (2005) 3812–3816.
[19] A. Stenberg, D. Malinovsky, B. Öhlander, H. Andrén, W. Forsling, L.-M. Engström, A. Wahlin, E. Engström, I. Rodushkin, D.C. Baxter, Measurement of iron and zinc isotopes in human whole blood: preliminary application to the study of HFE genotypes, J. Trace Elem. Med. Biol. 19 (2005) 55–60.
[20] Y. Anoshkina, M. Costas-Rodrıguez, M. Speeckaert, W. Van Biesen, J. Delanghe, F. Vanhaecke, Iron isotopic composition of blood serum in anemia of chronic kidney disease, Metall 9 (2017) 517–524.
[21] C. Weinstein, F. Moynier, K. Wang, R. Paniello, J. Foriel, J. Catalano, S. Pichat, Isotopic fractionation of Cu in plants, Chem. Geol. 286 (2011) 266–271.
[22] D. Jouvin, D.J. Weiss, T.F.M. Mason, M.N. Bravin, P. Louvat, F. Zhao, F. Ferec, P. Hinsinger, M.F. Benedetti, Stable isotopes of Cu and Zn in higher plants: evidence for Cu reduction at the root surface and two conceptual models for isotopic fractionation processes, Environ. Sci. Technol. 46 (2012) 2652–2660.
[23] K.A. Miller, F.A. Vicentini, S.A. Hirota, K.A. Sharkey, M.E. Wieser, Antibiotic treatment affects the expression levels of copper transporters and the isotopic composition of copper in the colon of mice, Proc. Natl. Acad. Sci. U.S.A. 116 (2019) 5955–5960.
[24] M. Costas-Rodríguez, S. Van Campenhout, A.A.M.B. Hastuti, L. Devisscher, H. Van Vlierberghe, F. Vanhaecke, Body distribution of stable copper isotopes during the progression of cholestatic liver disease induced by common bile duct ligation in mice, Metall 11 (2019) 1093–1103.
[25] K. Jaouen, M. Gibert, A. Lamboux, P. Télouk, F. Fourel, F. Albarède, A.N. Alekseev, E. Crubézy, V. Balter, Is aging recorded in blood Cu and Zn isotope compositions? Metall 5 (2013) 1016–1024.
[26] L. Sauzéat, A. Laurençon, V. Balter, Metallome evolution in ageing *C. elegans* and a copper stable isotope perspective, Metall 10 (2018) 496–503.
[27] M. Aramendia, L. Rello, M. Resano, F. Vanhaecke, Isotopic analysis of Cu in serum samples for diagnosis of Wilson's disease: a pilot study, J. Anal. At. Spectrom. 28 (2013) 675–681.
[28] M. Resano, M. Aramendía, L. Rello, M.L. Calvo, S. Bérail, C. Pécheyran, Direct determination of Cu isotope ratios in dried urine spots by means of fs-LA-MC-ICPMS. Potential to diagnose Wilson's disease, J. Anal. At. Spectrom. 28 (2013) 98–106.
[29] V. Balter, A. Nogueira da Costa, V.P. Bondanese, K. Jaouen, A. Lamboux, S. Sangrajrang, N. Vincent, F. Fourel, P. Télouk, M. Gigou, C. Lécuyer, P. Srivatanakul, C. Bréchot, F. Albarède, P. Hainaut, Natural variations of copper and sulfur stable isotopes in blood of hepatocellular carcinoma patients, Proc. Natl. Acad. Sci. U.S.A. 112 (2015) 982–985.
[30] L. Lobo, M. Costas-Rodríguez, J.C. de Vicente, R. Pereiro, F. Vanhaecke, A. Sanz-Medel, Elemental and isotopic analysis of oral squamous cell carcinoma tissues using sector-field and multi-collector ICP-mass spectrometry, Talanta 165 (2017) 92–97.
[31] M. Costas-Rodríguez, Y. Anoshkina, S. Lauwens, H. Van Vlierberghe, J. Delanghe, F. Vanhaecke, Isotopic analysis of Cu in blood serum by multi-collector ICP-mass spectrometry: a new approach for the diagnosis and prognosis of liver cirrhosis? Metall 7 (2015) 491–498.
[32] K.A. Miller, C.M. Keenan, G.R. Martin, F.R. Jirik, K.A. Sharkey, M.E. Wieser, The expression levels of cellular prion protein affect copper isotopic shifts in the organs of mice, J. Anal. At. Spectrom. 31 (2016) 2015–2022.
[33] T.G. Enge, H. Ecroyd, D.F. Jolley, J.J. Yerbury, A. Dosseto, Longitudinal assessment of metal concentrations and copper isotope ratios in the G93A SOD1 mouse model of amyotrophic lateral sclerosis, Metall 9 (2017) 161–174.
[34] F. Moynier, J. Creech, J. Dallas, M. Le Borgne, Serum and Brain natural copper stable isotopes in a mouse model of Alzeimer's disease, Sci. Rep. 9 (2019) 1–7.
[35] L. Sauzéat, E. Bernard, A. Perret-Liaudet, I. Quadrio, A. Vighetto, P. Krolak-Salmon, E. Broussolle, P. Leblanc, V. Balter, Isotopic evidence for disrupted copper metabolism in amyotrophic lateral sclerosis, iScience 6 (2018) 264–271.
[36] F. Moynier, S. Pichat, M.L. Pons, V. Balter, D. Fike, F. Albarède, Isotopic fractionation and transport mechanisms of Zn in plants, Chem. Geol. 267 (2009) 125–130.
[37] V. Balter, A. Zazzo, A. Moloney, F. Moynier, O. Schmidt, F. Monahan, F. Albarède, Bodily variability of zinc natural isotope abundances in sheep, Rapid Commun. Mass Spectrom. 24 (2010) 605–612.
[38] B. Mahan, F. Moynier, A.L. Jørgensen, M. Habekost, J. Siebert, Examining the homeostatic distribution of metals and Zn isotopes in Göttingen minipigs, Metall 10 (2018) 1264–1281.
[39] M. Costas-Rodríguez, L. Van Heghe, F. Vanhaecke, Evidence for a possible dietary effect on the isotopic composition of Zn in blood via isotopic analysis of food products by multi-collector ICP-mass spectrometry, Metall 6 (2014) 139–146.
[40] R.E.T. Moore, M. Rehkämper, W. Maret, F. Larner, Assessment of coupled Zn concentration and natural stable isotope analyses of urine as a novel probe of Zn status, Metall 11 (2019) 1506–1517.
[41] F. Moynier, J. Foriel, A.S. Shaw, M. Le Borgne, Distribution of Zn isotopes during Alzheimer's disease, Geochem. Perspect. Lett. 3 (2017) 142–150.
[42] F. Larner, L.N. Woodley, S. Shousha, A. Moyes, E. Humphreys-Williams, S. Strekopytov, A.N. Halliday, M. Rehkämper, R.C. Coombes, Zinc isotopic compositions of breast cancer tissue, Metall 7 (2015) 107–112.
[43] K. Schilling, F. Larner, A. Saad, R. Roberts, H.M. Kocher, O. Blyuss, A.N. Halliday, T. Crnogorac-Jurcevic, Urine metallomics signature as an indicator of pancreatic cancer, Metall 12 (2020) 752–757.
[44] A. Büchl, C.J. Hawkesworth, K.V. Ragnarsdottir, D.R. Brown, Re-partitioning of Cu and Zn isotopes by modified protein expression, Geochem. Trans. 9 (2008) 11.
[45] S.C. Yang, L. Welter, A. Kolatkar, J. Nieva, K.R. Waitman, K.F. Huang, W.H. Liao, S. Takano, W.M. Berelson, A.J. West, P. Kuhn, S.G. John, A new anion exchange purification method for Cu stable isotopes in blood samples, Anal. Bioanal. Chem. 411 (2019) 765–776.
[46] A. Stenberg, I. Malinovsky, I. Rodushkin, H. Andrén, C. Pontér, B. Öhlander, D. C. Baxter, Separation of Fe from whole blood matrix for precise isotopic ratio measurements by MC-ICP-MS: a comparison of different approaches, J. Anal. At. Spectrom. 18 (2003) 23–28.
[47] A. Stenberg, I.H. Andrén, I. Malinovsky, E. Engström, I. Rodushkin, D.C. Baxter, Isotopic variations of Zn in biological materials, Anal. Chem. 76 (2004) 3971–3978.
[48] S. Lauwens, M. Costas-Rodríguez, F. Vanhaecke, Ultra-trace Cu isotope ratio measurements via multi-collector ICP mass spectrometry using Ga as internal standard: an approach applicable to micro-samples, Anal. Chim. Acta 1025 (2018) 69–79.
[49] S. Lauwens, M. Costas-Rodríguez, H. Van Vlierberghe, F. Vanhaecke, Cu isotopic signature in blood serum of liver transplant patients: a follow-up study, Sci. Rep. 6 (2016) 30683.
[50] S. Lauwens, M. Costas-Rodríguez, H. Van Vlierberghe, F. Vanhaecke, High-precision isotopic analysis of Cu in blood serum via multi-collector ICP-mass spectrometry for clinical investigation: steps towards improved robustness and higher sample throughput, J. Anal. At. Spectrom. 32 (2017) 597–608.
[51] K. Sullivan, D. Layton-Matthews, M. Leybourne, J. Kidder, Z. Mester, L. Yang, Copper isotopic analysis in geological and biological reference materials by MC-ICP-MS, Geostand. Geoanal. Res. 44 (2) (2020) 349–362.
[52] R.E.T. Moore, F. Larner, B.J. Coles, M. Rehkämper, High precision zinc stable isotope measurement of certified biological reference materials using the double spike technique and multiple collector-ICP-MS, Anal. Bioanal. Chem. 409 (2017) 2941–2950.
[53] P.R. Craddock, N. Dauphas, Iron isotopic compositions of geological reference materials and chondrites, Geostand. Geoanal. Res. 35 (2011) 101–123.
[54] C.N. Maréchal, E. Nicolas, C. Douchet, F. Albarède, Abundance of zinc isotopes as a marine biogeochemical tracer, G-cubed 1 (2000), https://doi.org/10.1019/1999GC000029.
[55] T. Arnold, M. Schönbächler, M. Rehkämper, S. Dong, F.-J. Zhao, G.J.D. Kirk, B. J. Coles, D.J. Weiss, Measurement of zinc stable isotope ratios in biogeochemical matrices by double-spike MC-ICPMS and determination of the isotope ratio pool available for plants from soil, Anal. Bioanal. Chem. 398 (2010) 3115–3125.
[56] D.J. Weiss, N. Rausch, T.F.D. Mason, B.J. Coles, J.J. Wilkinson, L. Ukonmaanaho, T. Arnold, T.M. Nieminen, Atmospheric deposition and isotope biogeochemistry of zinc in ombrotrophic peat, Geochem. Cosmochim. Acta 71 (2007) 3498–3517.
[57] E. Smolders, L. Versieren, D. Shuofei, N. Mattielli, D. Weiss, I. Petrov, F. Degryse, Isotopic fractionation of Zn in tomato plants suggests the role of root exudates on Zn uptake, Plant Soil 370 (2013) 605–613.
[58] C. Caldelas, S. Dong, J.L. Araus, D.J. Weiss, Zinc isotopic fractionation in Phragmites australis in response to toxic levels of zinc, J. Experiment. Bot. 62 (2011) 2169–2178.
[59] J. Viers, P. Oliva, A. Nonell, A. Gélabert, J.E. Sonke, R. Freydier, R. Gainville, B. Dupré, Evidence of Zn isotopic fractionation in a soil–plant system of a pristine tropical watershed (Nsimi, Cameroon), Chem. Geol. 239 (2007) 124–137.
[60] C. Cloquet, J. Carignan, G. Libourel, Isotopic composition of Zn and Pb atmospheric depositions in an urban/periurban area of Northeastern France, Environ. Sci. Technol. 40 (2006) 6594–6600.
[61] L. Dinis, P. Gammon, M.M. Savard, C. Bégin, I. Girard, J. Vaive, Puzzling Zn isotopes in spruce tree-ring series, Chem. Geol. 476 (2018) 171–179.
[62] J.E. Sonke, Y. Sivry, J. Viers, R. Freydier, L. Dejong, L. André, J.K. Aggarwal, F. Fontan, B. Dupré, Historical variations in the isotopic composition of atmospheric zinc deposition from a zinc smelter, Chem. Geol. 252 (2008) 145–157.

[63] Y.-T. Tang, C. Cloquet, T. Sterckeman, G. Echevarria, J. Carignan, R.-L. Qiu, J.-L. Morel, Fractionation of stable zinc isotopes in the field-grown zinc hyperaccumulator *Noccaea caerulescens* and the zinc-tolerant plant silene vulgaris, Environ. Sci. Technol. 46 (2012) 9972–9979.
[64] C.N. Maréchal, P. Télouk, F. Albarède, Precise analysis of copper and zinc isotopic compositions by plasma-source mass spectrometry, Chem. Geol. 156 (1999) 251–273.
[65] M. Garçon, L. Sauzéat, R.W. Carlson, S.B. Shirey, M. Horan, M. Simon, V. Balter, M. Boyet, Nitrile, latex, neoprene and vinyl gloves: a primary source of contamination for trace element and Zn isotopic analyses in geological and biological samples, Geostand. Geoanal. Res. 41 (2017) 367–380.
[66] A. Vanderstraeten, S. Bonneville, S. Gili, J. de Jong, W. Debouge, P. Claeys, N. Mattielli, First multi-isotopic (Pb-Nd-Sr-Zn-Cu-Fe) characterisation of dust reference materials (ATD and BCR-723): a multi-column chromatographic method optimised to trace mineral and anthropogenic dust sources, Geostand. Geoanal. Res. 44 (2) (2020) 307–329.
[67] R Core Team, R: A Language and Environment for Statistical Computing, R Foundation for Statistical Computing, Vienna, Austria, 2013. http://www.R-project.org/.
[68] JCGM 100, Evaluation of Measurement Data – Guide to the Expression of Uncertainty in Measurement (ISO/IEC Guide 98-3).
[69] E.D. Young, A. Galy, H. Nagahara, Kinetic and equilibrium mass-dependent isotope fractionation laws in nature and their geochemical and cosmochemical significance, Geochem. Cosmochim. Acta 66 (2002) 1095–1104.